Propagation of gaseous detonation across inert layers

Yuan Wang[1,2], Chengyang Huang[2], Ralf Deiterding[3], Haitao Chen[1], Zheng Chen[2]*

[1] Key Laboratory of Computational Physics, Institute of Applied Physics and Computational Mathematics, Beijing 100094, China

[2] SKLTCS, CAPT, BIC-ESAT, College of Engineering, Peking University, Beijing 100871, China

[3] Aerodynamics and Flight Mechanics Research Group, University of Southampton, Boldrewood Campus, Southampton SO16 7QF, United Kingdom

Corresponding author: Zheng Chen, Ph.D.
State Key Laboratory for Turbulence and Complex Systems
Department of Mechanics and Engineering Science,
College of Engineering, Peking University
Beijing 100871, China
Tel: +86-(10) 6276-6232
Email: cz@pku.edu.cn

Colloquium topic: **Detonations, Explosions, and Supersonic Combustion**

Paper length (method 1):

Main Text:	word processor count	=	3487
Equations:	(1 line + 2) × (7.6 words/line) × (1 column)	=	15
References:	(33+2)×(2.3 lines/reference) × (7.6 words/line)	=	611
Figure Captions:	word processor count	=	290
Figure 1:	(45 mm+10) × (2.2 words/mm) × (2 column)	=	242
Figure 2:	(30 mm+10) × (2.2 words/mm) × (2 column)	=	176
Figure 3:	(52 mm+10) × (2.2 words/mm) × (1 column)	=	136
Figure 4:	(53 mm+10) × (2.2 words/mm) × (1 column)	=	138
Figure 5:	(49 mm+10) × (2.2 words/mm) × (1 column)	=	129
Figure 6:	(39 mm+10) × (2.2 words/mm) × (1 column)	=	107
Figure 7:	(147 mm+10) × (2.2 words/mm) × (1 column)	=	345
Figure 8:	(60 mm+10) × (2.2 words/mm) × (1 column)	=	154
Figure 9:	(33 mm+10) × (2.2 words/mm) × (1 column)	=	94
Figure 10:	(43 mm+10) × (2.2 words/mm) × (2 column)	=	233
	Total	**=**	**6157 words**

Supplementary Material: Yes (one file on grid convergence, density x-t diagram, critical inert layer thickness and independence of domain size)

Color reproduction: no (all color figures are to be printed in gray scale)

Propagation of gaseous detonation across inert layers

Yuan Wang[1,2], Chengyang Huang[2], Ralf Deiterding[3], Haitao Chen[1], Zheng Chen[2*]

[1] Key Laboratory of Computational Physics, Institute of Applied Physics and Computational Mathematics, Beijing 100094, China

[2] SKLTCS, CAPT, BIC-ESAT, College of Engineering, Peking University, Beijing 100871, China

[3] Aerodynamics and Flight Mechanics Research Group, University of Southampton, Boldrewood Campus, Southampton SO16 7QF, United Kingdom

Abstract

In rotating detonation engines and explosion accidents, detonation may propagate in an inhomogeneous mixture with inert layers. This study focuses on detonation propagation in a stoichiometric $H_2/O_2/N_2$ mixture with multiple inert layers normal to the detonation propagation direction. One- and two-dimensional simulations considering detailed chemistry are conducted. The emphasis is placed on assessing the effects of inert layer on detonation reinitiation/failure, detonation propagation speed, detonation cell structure and cell size. Specifically, the inert layer thickness and the spacing between two consecutive inert layers are varied. Either detonation reinitiation or failure across the inert layers is observed. It is found that successful detonation reinitiation occurs only at relatively small values of the inert layer thickness and spacing. For each given value of the inert layer spacing, there is a critical inert layer thickness above which detonation fails after crossing the inert layers. This critical inert layer thickness is found to decrease as the inert layer spacing increases. The detailed process of detonation reinitiation across the inert layers is analyzed. The interaction between the transverse shock waves is shown to induce local autoignition/explosion and eventually over-driven detonation development in the reactive layer. The averaged detonation propagation speed in the inhomogeneous mixture is compared to the CJ speed and very good agreement is achieved. This indicates that the inert layer does not affect the detonation propagation speed once successful detonation reinitiation happens. Unlike the detonation speed, the detonation cell structure and cell size are greatly affected by the inert layer results. For the first time, large cellular structure with size linearly proportional to the inert layer spacing is observed for detonation propagation across inert layers. Besides, a double cellular structure is observed for relatively large spacing between inert layers. The formation of double cellular structure is interpreted.

Keywords: Detonation propagation; inhomogeneous mixture; inert layer; cell structure

* Corresponding author. E-mail: cz@pku.edu.cn

1. Introduction

Recently, substantial progress has been made in understanding gaseous detonation because it has promising application in propulsion and it might occur in accidental explosions. Though previous studies mainly focused on detonation propagation in homogenous combustible mixtures, in practice gaseous detonation may propagate in an inhomogeneous mixture. For examples, in rotating detonation engines (RDEs) the fuel and oxidizer are generally injected separately into the chamber and might not be perfectly mixed [1-3]; and in explosion accidents inert mixtures are injected to damp/suppress detonation [4]. Therefore, it is necessary to understand the properties of gaseous detonation propagating in inhomogeneous mixtures.

In the literature, several studies on detonation propagating in inhomogeneous mixtures have been reported. Figure 1 shows the four typical cases considered in previous studies: reactants with fuel concentration gradient (a) normal (e.g., [5, 6]) and (b) parallel [7, 8] to the detonation propagation direction; and reactants with inert layers (c) parallel [9, 10] and (d) normal [2-4, 11-13] to the detonation propagation direction. Besides, other inhomogeneous mixtures were also studied previously [14-17].

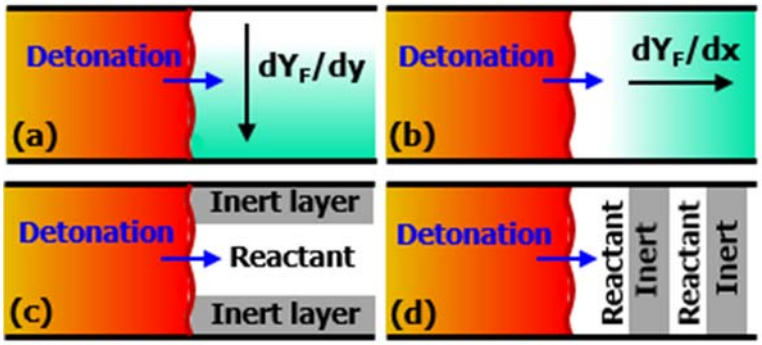

Fig. 1. Schematic of detonation propagating in four types of inhomogeneous mixture.

This work focuses on detonation propagation across inert layers as shown in Fig. 1(d). In RDEs, burned gas might appear between fresh mixtures due to the injection nozzle interval [1-3]. Therefore, the case depicted in Fig. 1(d) is relevant to combustion in RDEs. Furthermore, it's also closely related to detonation suppression and reinitiation in explosion accidents [4]. Previous studies on this type of inhomogeneous mixture are briefly introduced here. Bjerketvedt et al. [11]

experimentally studied the reinitiation of detonation across a single inert layer. They found that the reinitiation is determined by the shock strength of the initial detonation, the inert layer thickness and the reactivity of the mixture after the inert layer. Teodorczyk and Benoan [12] conducted experimental and numerical studies on detonation interaction with an inert gas zone. They considered and compared different types of inert gas (Ar, He, N_2 and CO_2) in terms of detonation damping. Ishii and Seki [4] experimentally investigated the behavior of detonation transmission into inert gas zones and found that the length of the inert gas zone greatly affects the propagation of the transmitted shock wave and flame front. Fujii et al. [2] and Chen et al. [3] conducted two-dimensional (2D) simulations and found that the mixture non-uniformity due to discrete injections reduces detonation velocity and induces mode switching in RDEs. Tang-Yuk et al. [13] simulated detonation across a single inert layer and found that the critical inert layer thickness for successful reinitiation in 2D case is an order of magnitude larger than that in the one-dimensional (1D) case.

Most of the studies mentioned above considered one single inert layer and focused on the critical inert layer thickness for detonation reinitiation. However, the influence of inert layers on the detonation cell structure and size received little attention. Moreover, previous studies mainly used one-step chemistry in simulation, which was not appropriate for detonation reinitiation due to the absence of the cross-over temperature [18]. Based on these considerations, here we consider detonation propagation in a stoichiometric $H_2/O_2/N_2$ mixture with multiple inert layers. The objective is to examine the effects of inert layers on detonation reinitiation, cell structure, cell size and detonation propagation speed. Both 1D and 2D simulations are conducted. Detailed chemistry and diffusive transport are accurately considered in the simulations.

2. Numerical model and methods

We consider 1D and 2D detonation propagation in a stoichiometric $H_2/O_2/N_2$ mixture with inert layers. The ZND detonation structure with the induction length of l_i is simulated by Cantera [19]. As sketched in Fig. 2, the distributions of pressure, temperature, and mass fractions of all species from the ZND structure are used as the initial conditions in the left part of the computational domain

to initiate detonation. The detonation first propagates through a static, homogeneous, stoichiometric H_2/air mixture, in which the cell structure fully develops in the 2D case. Then it propagates into the static inhomogeneous mixture with inert and reactive layers appearing alternatively.

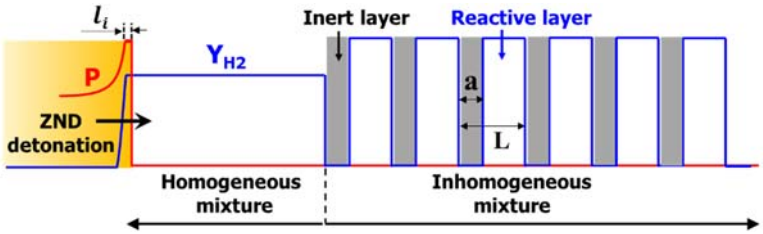

Fig. 2. Schematic of the initial pressure and hydrogen mass fraction distributions and the inert and reactive layers.

The stoichiometric H_2/air (i.e., H_2:O_2:N_2=2:1:3.76) is uniformly distributed in homogeneous domain. In inhomogeneous domain, the inert layer thickness is a and the spacing between two consecutive inert layers is L. The inert layer consists of pure nitrogen. The molar ratio in the reactive layer is H_2:O_2:N_2=2:1:x where x is to be determined. In order to fairly compare the results between the homogeneous and inhomogeneous mixtures, the averaged H_2 concentration in the inhomogeneous mixture is the same as that in the homogeneous mixture with the following relationship:

$$\frac{2}{(2+1+3.76)}L = 0\cdot a + \frac{2}{(2+1+x)}\cdot(L-a) \tag{1}$$

Rearrangement of the above equation yields x=3.76-6.76a/L. To ensure $x \geqslant 0$, we have $a/L \leqslant 0.556$. Different values of L in the range of 0~8 mm and a in the range of 0~1 mm are considered here. The homogeneous mixture is recovered for a=0 mm. All the unburned mixtures are initially at T_0=300 K and P_0=1 atm. Adiabatic and reflective wall boundary conditions are used for the left and right sides in both 1D and 2D simulations. Periodic boundary conditions are used for the top and bottom sides in 2D simulations.

The in-house code A-SURF [20-22] and the parallel block-structured mesh refinement framework AMROC [23] are respectively used to simulate 1D and 2D detonation propagating across inert layers. The conservation equations for unsteady, compressible, multi-component, reactive flow are solved in A-SURF and AMROC using the finite volume method. Diffusion terms are kept in the

conservation equations. The CHEMKIN package is used to evaluate the thermodynamic and transport properties as well as the reaction rates. The hydrogen chemistry developed by Li et al. [24] is used. Both A-SURF and AMROC were successfully used in previous studies on detonation initiation and propagation (e.g. [23, 25-28]). The details on governing equations and numerical schemes of A-SURF and AMROC can be found in [20-23].

To accurately and efficiently resolve the propagating shock and reaction zone as well as the interface between the inert and reactive layers, dynamically adaptive mesh refinement is used both in 1D and 2D simulations. Mesh refinement or coarsening is determined by the local temperature and pressure gradients. The finest mesh size is 3.9 μm. Since the detonation induction length is l_i = 0.19 mm, there are more than 45 mesh points within one induction length. The grid convergence is ensured, which is demonstrated in the Supplementary Document.

3. Results and discussion

3.1 One-dimensional detonation propagation

First we consider 1D detonation propagating across inert layers with different values of thickness or spacing. The first inert layer starts at $x_{\text{start,1D}}$=8 cm and the homogeneous mixture is within the region of $0 \le x \le 8$ cm. The computational domain is $0 \le x \le 20$ cm. For simplicity, here we only consider the case with only one inert layer.

Figure 3 shows the evolution of the leading shock speed for different values of spacing and thickness of the inert layer. In the inert layer, the shock wave decouples from the original detonation and decelerates. Detonation reinitiation downstream the inert layer can be induced by the transmitted shock if it is strong enough.

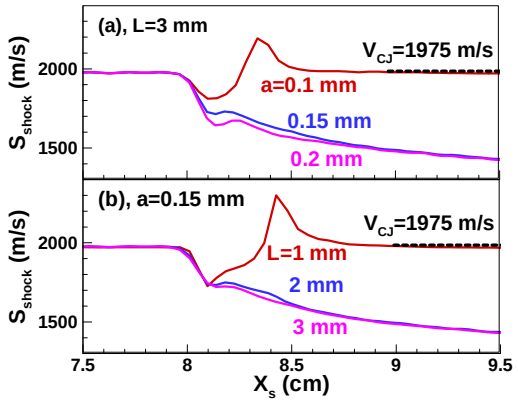

Fig. 3. Change of the leading shock speed, S_{shock}, with its position, X_s, for (a) fixed L=3 mm and different values of a; (b) fixed a=0.15 mm and different values of L.

It is observed that detonation reinitiation occurs only for (a) small thickness of a=0.1 mm with fixed spacing of L=3 mm and (b) small spacing of L=1 mm with fixed thickness of a=0.15 mm. Across the inert layer, the shock speed decays from 1975 m/s (CJ speed) to 1818 m/s for a=0.1 mm and 1650 m/s for a=0.2 mm. The relatively stronger transmitted shock for a=0.1 mm helps to achieve detonation reinitiation as shown in Fig. 3(a). An over-driven detonation is first produced and then it decays to a CJ detonation. There is a critical inert layer thickness, denoted as a_c, and successful detonation reinitiation can be achieved only for $a<a_c$. For a fixed inert layer thickness of a=0.15 mm, the nitrogen concentration in the reactive layers decreases as the spacing decreases since H_2:O_2:N_2=2:1:(3.76-6.76a/L). Consequently, as shown in Fig. 3(b), detonation reinitiation happens for L=1 mm but not for L=2 and 3 mm. Therefore, detonation reinitiation only occurs for relatively small values of a and L, respectively corresponding to a stronger transmitted shock and a higher reactivity of the mixture after the inert layer. This is consistent with the results of Bjerketvedt et al. [11].

To interpret the detonation-inert layer interaction, we plot the density contour in the x-t diagram for L=3 mm and a=0.15 mm in Fig. 4. The detonation propagates in a homogeneous mixture before it collides with the inert layer starting at $x_{start,1D}$=8 cm. For x<8 cm, the shock couples with the reaction zone (yellow region in Fig. 4). Figure 4 shows that the interaction between the initial

detonation and inert layer results in a transmitted shock, a contact surface and a reflected rarefaction wave. The transmitted shock induces chemical reaction in the reactive layer. However, the reaction zone decouples from the shock and their distance is shown to increase with time. Therefore, detonation reinitiation fails. For successful detonation reinitiation, the reaction zone needs to remain connected to the transmitted shock across the inert layer (see Fig. S3 in the Supplementary Document).

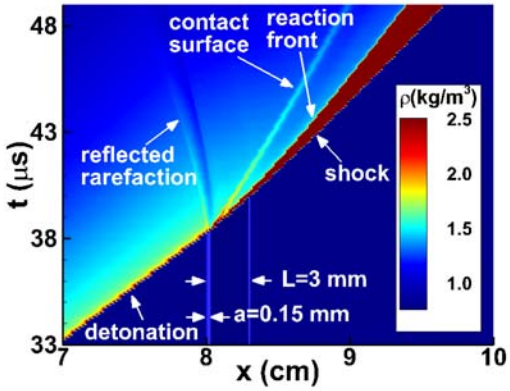

Fig. 4. Density contour in the *x*-*t* diagram. The two vertical blue lines represent inert layers with L=3 mm and a=0.15 mm.

Figure 5 plots the normalized critical inert layer thickness and the normalized detonation propagation speed. The upper limit of a_c/L=0.556 is to ensure that the nitrogen concentration in the reactive layer is not negative (see Section 2). Both a_c/L and a_c (not shown here) decrease with the increase of L. This is because for larger L the reactive mixture consists of more nitrogen and thereby has lower reactivity. For L>5 mm, a_c approaches a constant value, which is the critical thickness for the case with one single inert layer. Note that the number of inert layer has little influence on the critical thickness (which is demonstrated in Fig. S4 in the Supplementary Document). Moreover, Fig. 5 shows that the appearance of inert layers has little influence on the averaged detonation speed once successful reinitiation is achieved. The difference between the detonation speeds in the inhomogeneous and homogeneous mixtures is less than 1%. A similar observation was found in [14].

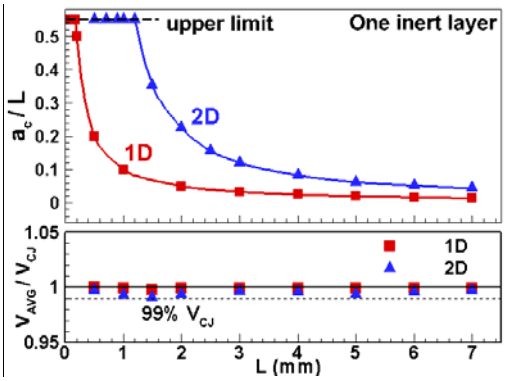

Fig. 5. Change of the normalized critical inert layer thickness a_c/L (top) and normalized averaged detonation propagation speed V_{AVG}/V_{CJ} (bottom) versus the spacing between two inert layers, L.

3.2 Two-dimensional detonation propagation

Here we consider 2D detonation propagation across multiple inert layers. The first inert layer starts at $x_{start,2D}$=6 cm. In the homogeneous mixture within the region of $0 \le x \le 6$ cm, the detonation cellular structure is fully developed. The whole computational domain is 30 cm×3 cm.

Figure 6 shows the numerical soot foils for fixed spacing but different values of inert layer thickness. For a=0 mm (i.e., homogeneous mixture without inert layers), the detonation propagates at the C-J speed and has regular cellular structure. The cell size (height in the vertical direction) is about 0.4 mm. For a=0.15 and 0.3 mm, successful detonation reinitiation is achieved in the inhomogeneous mixture and large regular cellular structures are observed after a transition region at $6 \le x \le 8.5$ cm and $6 \le x \le 7.5$ cm for a=0.15 and 0.3 mm, respectively. For both a=0.15 and 0.3 mm, the size of the large cellular structure is around 2.6 mm, which is about six times of the original cell size in the homogeneous mixture. Therefore, the size of the large cellular structure is independent of the inert layer thickness once detonation reinitiation happens. Figure 6 shows that further increase of the inert layer thickness to a=0.4 mm results in detonation quenching.

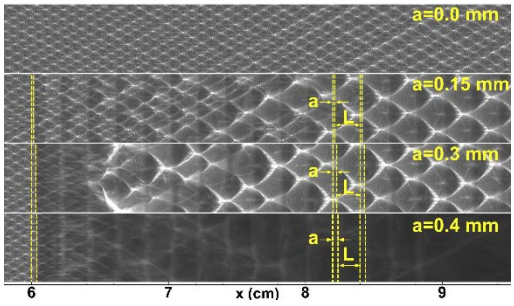

Fig. 6. Numerical soot foils for fixed spacing of L=2 mm and different inert layer thicknesses of a=0, 0.15, 0.3 and 0.4 mm.

The critical inert layer thickness for this 2D case is a_c=0.37 mm, which is much larger than a_c=0.1 mm for the same spacing of L=2 mm in the 1D case. This is similar to the results of Tang-Yuk et al. [13] who found in their simulations that critical inert layer thickness in 2D case is an order of magnitude larger than that in the 1D case considering simplified three-step chemistry. Figure 5 compares the critical inert layer thickness from 1D and 2D simulations. As expected, for a given inert layer spacing, the critical inert layer thickness for successful detonation reinitiation in the inhomogeneous mixture for the 2D case is much larger than that for the 1D case. In the 1D case, there is only a transmitted normal shock which induces chemical reaction in the reactive layers. However, in the 2D case there are Mach stem, transverse and incident shock waves, and their interaction can induce strong local autoignition and explosion, which will be shown later. Moreover, Fig. 5 shows that the averaged detonation speed in both 1D and 2D cases are nearly the same as the CJ detonation speed once successful detonation reinitiation is achieved. It is noted that here the averaged hydrogen concentration in the inhomogeneous mixture is the same as that in the homogeneous mixture (see Fig. 2 and related description). If the local hydrogen concentration in the reactive layer is the same as that in the homogeneous mixture, the averaged detonation speed in the inhomogeneous mixture will be lower than the CJ detonation speed due to the presence of the inert layers.

To interpret the reinitiation process in the inhomogeneous mixture, we plot the evolution of temperature and inert gas mass fraction distributions in Fig. 7. Figure 7(a) shows the shock across the first three inert layers for L=2 mm and a=0.3 mm. At t=29 μs, the detonation propagates in the homogenous mixture and the original triple points can be observed. At t=29.7 μs, the detonation

collides with the first inert layer and the leading shock decouples with the reaction zone. Therefore, the detonation is quenched and only the leading shock propagates across the inert layer. At t=30.3 μs, the transmitted shock propagates into the first reactive layer and it compresses the $H_2/O_2/N_2$ mixture therein. The transverse waves moving with the original triple points further compress the reactive mixture and eventually triggers local autoignition occurring at the location where two transverse waves collide [6]. The rapid heat release from the local autoignition leads to the generation of a pressure wave, which further compresses the unburned gas and induces further autoignition. Consequently, global autoignition is shown to occur at t=31.2 μs, and meanwhile the leading shock is shown to reach the second inert layer. At t=31.7 μs, the leading shock propagates into the second reactive layer and local explosions occur immediately behind the leading shock. Consequently, detonation reinitiation is achieved due to the coherent coupling between autoignition and pressure wave. Though reactivity gradient is not specified initially, it can be developed during the shock propagation and thereby the detonation reinitiation is consistent with the SWACER (Shock-Wave Amplification by Coherent Energy Release) mechanism [29]. A similar phenomenon was observed in experiments [30]. Therefore, detonation quenching and reinitiation occur alternatively in the first several inert and reactive layers. After the transition, quasi-steady detonation propagation occurs in the inhomogeneous mixture with x>7.5 cm.

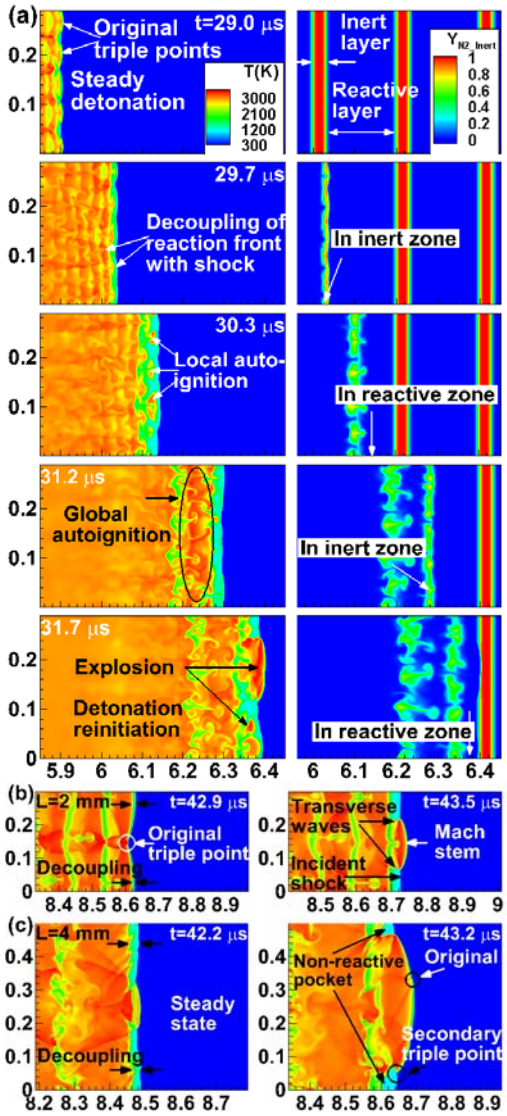

Fig. 7. (a) Evolution of temperature (left) and inert gas mass fraction (right) contours for L=2 mm and a=0.3 mm within the transition region; evolution of temperature contour for (b) L=2 mm and a=0.3 mm and (c) L=4 mm and a=0.3 mm in the steady state. The label of both axes is in the unit of centimeter.

The quasi-steady detonation propagating in the inhomogeneous mixture is shown in Figs. 7(b) and 7(c) for the same a=0.3 mm but different values of L=2 and 4 mm. At t=42.9 μs, the detonation propagates across the thirteenth inert layer starting at x=8.6 cm for L=2 mm. As the detonation propagates forward, the transverse waves collide near the center line at y=0.15 cm and then propagate towards up and down sides. The coupling between the leading shock (i.e., strong Mach stem) and the reaction zone forms the overdriven detonation, behind which the fresh mixtures from the previous reactive layer are compressed into the inert layer and are fully consumed near the triple points.

However, at the vicinity of top and bottom boundary, the distance of the leading shock (i.e., weak incident shock) and reaction zone becomes large. Especially at t=43.5 μs it reaches about 0.4 mm, which is much longer than the induction length of l_i=0.19 mm. The temperature behind the leading shock is lower than 1000 K. This region is defined as the non-reactive pocket [15] and the leading shock is defined as the inert normal shock [6]. This observation is different from detonation propagation across a homogeneous mixture. Here, the inert layer causes obvious decoupling between the leading shock and reaction zone when the detonation propagates across the inhomogeneous mixture. For L=4 mm, a similar process of detonation propagation can be observed. However, the original and secondary triple points are shown to coexist at t=43.2 μs. This generates double cellular structures to be discussed later.

Figures 8 and 9 show the effects of inert layer spacing on the detonation cellular structure and cell size in the inhomogeneous mixture. Steady detonation propagation in the inhomogeneous mixture is achieved for x>8 cm. Figure 8 shows that when the inert layer spacing is increased from L=2 mm to L=4 mm, the large cell size doubles. Moreover, for L=4 mm, a substructure within the large cellular structure is observed. This is similar to the double cellular structure observed in a gaseous nitromethane/air mixture [31]. However, the mechanisms of forming such kind of double cellular structure are different. For the nitromethane/air mixture, the double cellular structure is associated with the two characteristic induction lengths due to two-stage heat release of nitromethane [32]. Here the large cellular structure is associated with the inert layer spacing while the substructure is associated with the induction length of the $H_2/O_2/N_2$ mixture. The regular movement of original triple points generate the substructure whose size is nearly the same as that in a homogeneous mixture. The large cellular structure is formed by the secondary triple points, resulting from the local explosion shown in Fig. 5(a). Such interesting cellular structure was also obtained by Radulescu and Mawell [17] in their studies on detonation attenuation and reinitiation across a porous section consisting of staggered cylinders. It is noted that such kind of cell-bifurcation was also observed in cylindrical detonation by Asahara et al. [33].

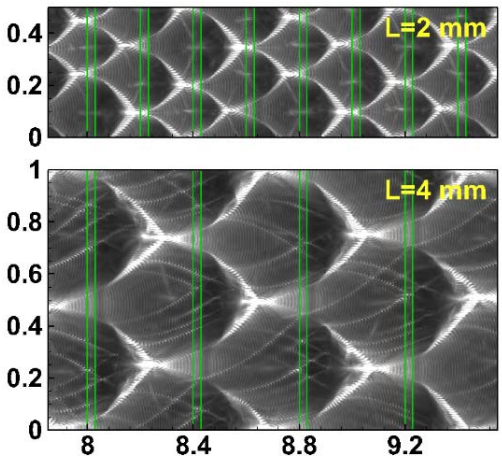

Fig. 8. Numerical soot foils for fixed inert layer thickness of a=0.3 mm and different spacing of L=2 and 4 mm. The inert layers are between a pair of vertical green lines whose distance is 0.3 mm. The label of both axes is in the unit of centimeter.

Figure 9 shows that the global cell size increases linearly with the inert layer spacing, L. This further confirms that the large cellular structure is associated with the inert layer spacing. Therefore, the cell size for detonation propagation in an inhomogeneous mixture with inert layers is independent of the inert layer thickness (see Fig. 6) and it is linearly proportional to the inert layer spacing. Note that Fig. S5 in the Supplementary Document the global cell size does not change with computational domain size.

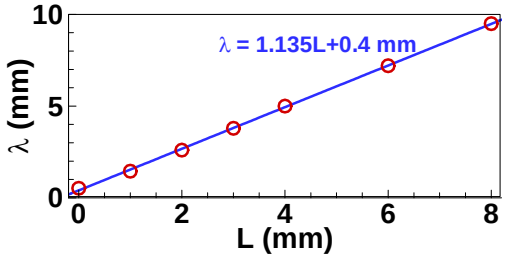

Fig. 9. Change of the global cell size, λ, with the spacing between two consecutive inert layers, L. The symbols are simulation results; and the line is a linear fit.

The enlarged cellular structure in the inhomogeneous mixture is shown in Fig. 10. The yellow lines represent the trajectories of the secondary triple points, at which the incident shock, Mach stem and transverse wave collide with one another. A complete cellular structure forms between two consecutive collisions of a pair of transverse waves occurring at points A and B in Fig. 10. The pair

of transverse waves propagates in the opposite directions until the reflection at points C and D due to the collision with other transverse waves. Then these two transverse waves propagate toward each other and collide at point B. It is found that the original triple points are located at the fronts of incident shock and Mach stem. The original and secondary triple points generate substructure and large cellular structure, respectively.

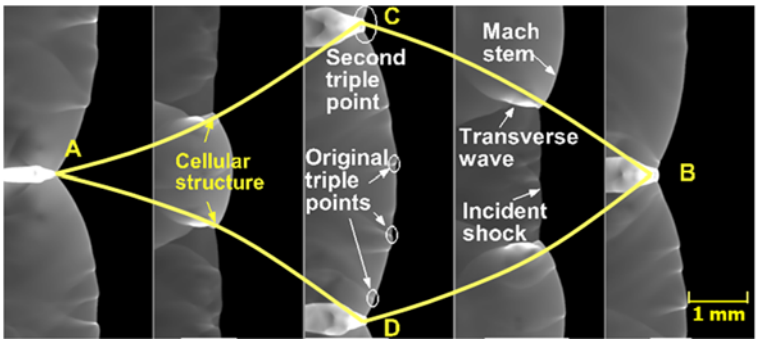

Fig. 10. The pressure contours at five instants which form a large cellular structure for a=0.3 mm and L=4 mm.

4. Conclusions

One- and two-dimensional simulations considering detailed chemistry have been conducted for detonation propagation in a stoichiometric $H_2/O_2/N_2$ mixture with multiple inert layers. The detonation first propagates in the homogeneous mixture, and then it propagates into the inhomogeneous mixture with inert and reactive layers appearing alternatively. Depending on the inert layer thickness and the spacing between two consecutive inert layers, either detonation reinitiation or failure occurs in the inhomogeneous mixture. For successful detonation reinitiation across the inert layers, detonation quenching, autoignition, local explosion and over-driven detonation development occur alternatively in the first several inert and reactive layers. It is found that successful detonation reinitiation occurs only for relatively small inert layer thickness and spacing. As inert layer spacing increases, the critical inert layer thickness first rapidly decreases and then it approaches a nearly constant value. The critical inert layer thickness for the 2D case is found to be much larger than that for the 1D case due to the cellular structure with triple points in the 2D case. The inert layer does not affect the averaged detonation propagation speed once successful detonation reinitiation is achieved.

However, the inert layer results in large cellular structure whose size is linearly proportional to the inert layer spacing. Besides, the double cellular structure (i.e., substructure inside a large cellular structure) is observed when the spacing between inert layers is large enough. The original and secondary triple points respectively generate the substructure and large cellular structure.

It is noted that the simplified model considered here is not like the case in RDEs [2] since the inert gas is not the hot product and its motion is not considered. The effects of the thermal and hydrodynamic properties of the mixture in the inert layers need to be explored in future studies. Besides, the mixture composition distributions close to the practical cases in RDEs deserve further study.

Acknowledgements

This work was supported by the National Natural Science Foundation of China (Nos. 91741126 and 51861135309). Y.W. and Z.C. thank Dr. Xiaocheng Mi at University of Cambridge for helpful discussion. The simulations were conducted on the High Performance Computing Platform of the Center for Life Science at PKU.

References

[1] F. K. Lu, E. M. Braun, Rotating detonation wave propulsion_ experimental challenges, modeling, and engine concepts, J. Propul. Power 30 (2014) 1125-1142.

[2] J. Fujii, Y. Kumazawa, A. Matsuo, S. Nakagami, K. Matsuoka, J. Kasahara, Numerical investigation on detonation velocity in rotating detonation engine chamber, Proc. Combust. Inst. 36 (2017) 2665-2672.

[3] Y. L. Chen, X. Y. Liu, J. P. Wang, Mode switching in 2-dimensional continuous detonation chambers with discrete injectors, Proceedings of the 27th International Colloquium on the Dynamics of Explosions and Reactive Systems, Beijing, 2019.

[4] K. Ishii, K. Seki, A study on suppression of detonation propagation by inert gas injection, Proceedings of the 27th International Colloquium on the Dynamics of Explosions and Reactive Systems, Beijing, 2019.

[5] K. Ishii, M. Kojima, Behavior of detonation propagation in mixtures with concentration gradients, Shock Waves 17 (1-2) (2007) 95-102.

[6] D. A. Kessler, V. N. Gamezo, E. S. Oran, Gas-phase detonation propagation in mixture composition gradients, Philos Trans A Math Phys Eng Sci 370 (1960) (2012) 567-596.

[7] M. S. Kuznetsov, V. I. Alekseev, S. B. Dorofeev, I. D. Matsukov, J. L. Boccio, Detonation propagation, decay, and reinitiation in nonuniform gaseous mixtures, Proc. Combust. Inst. 27 (1998) 2241-2247.

[8] S. Boulal, P. Vidal, R. Zitoun, Experimental investigation of detonation quenching in non-uniform compositions, Combust. Flame 172 (2016) 222-233.

[9] M. Reynaud, F. Virot, A. Chinnayya, A computational study of the interaction of gaseous detonations with a compressible layer, Phys. Fluids A 29 (2017) 056101.

[10] R. W. Houim, R. T. Fievisohn, The influence of acoustic impedance on gaseous layered detonations bounded by an inert gas, Combust. Flame 179 (2017) 185-198.

[11] D. Bjerketvedt, O. K. Sonju, I. O. Moen, The influence of experimental condition on the reinitiation of detonation across an inert region, Progress in Astronautics and Aeronautics 106 (1986) 109-130.

[12] A. Teodorczyk, F. Benoan, Interaction of detonation with inert gas zone, Shock Waves 6 (4) (1996) 211-223.

[13] K. C. Tang Yuk, J. H. S. Lee, H. D. Ng, X. Mi, Detonation transmission across an inert gap, Proceedings of the 27th International Colloquium on the Dynamics of Explosions and Reactive Systems, Beijing, 2019.

[14] J. Li, X. Mi, A. J. Higgins, Effect of spatial heterogeneity on near-limit propagation of a pressure-dependent detonation, Proc. Combust. Inst. 35 (2) (2015) 2025-2032.

[15] X. Mi, A. J. Higgins, H. D. Ng, C. B. Kiyanda, N. Nikiforakis, Propagation of gaseous detonation waves in a spatially inhomogeneous reactive medium, Physical Review Fluids 2 (5) (2017) 053201.

[16] A. V. Gaathaug, K. Vaagsaether, D. Bjerketvedt, Detonation failure in stratified layers-the influence of detonation regularity, Proceedings of the 26th International Colloquium on the Dynamics of Explosions and Reactive Systems, Boston, 2017.

[17] M. I. Radulescu, B. M. Maxwell, The mechanism of detonation attenuation by a porous medium and its subsequent re-initiation, J. Fluid Mech. 667 (2011) 96-134.

[18] J. H. S. Lee, A. J. Higgins, Comments on criteria for direct initiation of detonation, Philosophical Transactions of the Royal Society of London A: Mathematical, Physical and Engineering Sciences 357 (1999) 3503-3521.

[19] D. Goodwin, H. K. Moffat, R. L. Speth, Cantera: an object-oriented software toolkit for chemical kinetics, thermodynamics, and transport processes, Caltech, Pasadena, CA, 2009.

[20] Z. Chen, M. P. Burke, Y. Ju, Effects of Lewis number and ignition energy on the determination of laminar flame speed using propagating spherical flames, Proc. Combust. Inst. 32 (1) (2009) 1253-1260.

[21] Z. Chen, Effects of radiation and compression on propagating spherical flames of methane/air mixtures near the lean flammability limit, Combust. Flame 157 (12) (2010) 2267-2276.

[22] P. Dai, Z. Chen, Supersonic reaction front propagation initiated by a hot spot in n -heptane/air mixture with multistage ignition, Combust. Flame 162 (11) (2015) 4183-4193.

[23] R. Deiterding, A parallel adaptive method for simulating shock-induced combustion with detailed chemical kinetics in complex domains, Computers & Structures 87 (11-12) (2009) 769-783.

[24] J. Li, Z. Zhao, A. Kazakov, F. L. Dryer, An updated comprehensive kinetics model of hydrogen combustion, Int. J. Chem. Kinet. 36 (10) (2004) 566-575.

[25] C. Qi, Z. Chen, Effects of temperature perturbation on direct detonation initiation, Proc. Combust. Inst. 36 (2) (2017) 2743-2751.

[26] C. Huang, C. Qi, Z. Chen, Non-uniform ignition behind a reflected shock and its influence on ignition delay measured in a shock tube, Shock Waves 29 (7) (2019) 957-967.

[27] Y. Wang, W. Han, R. Deiterding, Z. Chen, Effects of disturbance on detonation initiation in $H_2/O_2/N_2$ mixture, Physical Review Fluids 3 (12) (2018) 123201.

[28] R. Deiterding, High-resolution numerical simulation and analysis of Mach reflection structures in detonation waves in low-rpessure H_2-O_2-Ar mixtures: A summary of results obtained with the adaptive mesh refinement framework AMROC, Journal of Combustion 2011 (2011) 1-18.

[29] J. H. Lee, The detonation phenomenon, Cambridge University Press Cambridge, 2008.

[30] J. Li, W. H. Lai, K. Chung, F. K. Lu, Experimental study on transmission of an overdriven detonation wave from propane/oxygen to propane/air, Combust. Flame 154 (3) (2008) 331-345.

[31] H. N. Presles, D. Desbordes, M. Guirard, C. Guerraud, Gaseous nitromethane and nitromethane-oxygen mixtures: A new detonation structure, Shock Waves 6 (2) (1996) 111-114.

[32] M. Faghih, Z. Chen, Two-stage heat release in nitromethane/air flame and its impact on laminar flame speed measurement, Combust. Flame 183 (2017) 157-165.

[33] M. Asahara, N. Tsuboi, A. K. Hayashi, E. Yamada, Two-dimensional simulation on propagation mechanism of H_2/O_2 cylindrical detonation with a detailed reaction model: influence of initial energy and propagation mechanism, Combust. Sci. Technol. 182 (11-12) (2010) 1884-1900.

Figure captions

Fig. 1. Schematic of detonation propagating in four types of inhomogeneous mixture.

Fig. 2. Schematic of the initial pressure and hydrogen mass fraction distributions and the inert and reactive layers.

Fig. 3. Change of the leading shock speed, S_{shock}, with its position, X_s, for (a) fixed L=3 mm and different values of a; (b) fixed a=0.15 mm and different values of L.

Fig. 4. Density contour in the x-t diagram. The two vertical blue lines represent inert layers with L=3 mm and a=0.15 mm.

Fig. 5. Change of the normalized critical inert layer thickness a_c/L (top) and normalized averaged detonation propagation speed V_{AVG}/V_{CJ} (bottom) versus the spacing between two inert layers, L.

Fig. 6. Numerical soot foils for fixed spacing of L=2 mm and different inert layer thicknesses of a=0, 0.15, 0.3 and 0.4 mm.

Fig. 7. (a) Evolution of temperature (left) and inert gas mass fraction (right) contours for L=2 mm and a=0.3 mm within the transition region; evolution of temperature contour for (b) L=2 mm and a=0.3 mm and (c) L=4 mm and a=0.3 mm in the steady state. The label of both axes is in the unit of centimeter.

Fig. 8. Numerical soot foils for fixed inert layer thickness of a=0.3 mm and different spacing of L=2 and 4 mm. The inert layers are between a pair of vertical green lines whose distance is 0.3 mm. The label of both axes is in the unit of centimeter.

Fig. 9. Change of the global cell size, λ, with the spacing between two consecutive inert layers, L. The symbols are simulation results; and the line is a linear fit.

Fig. 10. The pressure contours at five instants which form a large cellular structure for a=0.3 mm and L=4 mm.